Calcolo (2026) 63:16
https://doi.org/10.1007/s10092-026-00690-3

Robust Arrow–Hurwicz method for high–Rayleigh number Boussinesq flow

Aziz Takhirov[1] · Mustafa Aggul[2,3,4] · Sinan Ergen[5,6] · Fatma G. Eroglu[7] · Songül Kaya[8]

Received: 13 November 2025 / Revised: 26 February 2026 / Accepted: 4 March 2026

Abstract
We develop and analyze a robust Arrow–Hurwicz (AH) iterative method for the numerical solution of steady Boussinesq flows with nonhomogeneous partitioned Dirichlet boundary conditions. Although a direct AH formulation may be applied to the momentum equation alone, we demonstrate that incorporating an AH-type update for the temperature equation is crucial for stability and convergence in buoyancy-driven systems, particularly at high Rayleigh numbers. The resulting Improved Arrow–Hurwicz (IAH) scheme avoids solving saddle-point systems at each iteration and yields a fully decoupled algorithm with low computational cost per step. We establish existence, uniqueness, uniform boundedness, and convergence under standard small-data assumptions, and provide corresponding error estimates for the finite element discretization. Extensive two- and three-dimensional numerical experiments verify the theoretical findings, demonstrate significant acceleration over the alternative AH scheme and the Penalty–Picard iteration, and confirm robust convergence in high–Rayleigh number regimes. The proposed method offers a scalable and efficient solver for steady natural convection and provides a promising alternative to continuation-based approaches traditionally used for high–Rayleigh flows.

Keywords Arrow–Hurwicz method · High Rayleigh number · Penalty–Picard iteration · Boussinesq flow · Differentially heated cavity

1 Introduction

The goal of this study is to extend the novel approximation framework introduced in [33] to the steady-state Boussinesq equations with non-homogeneous, partitioned Dirichlet boundary conditions. We consider the system over a domain $\Omega \subset \mathbb{R}^d$, $d \in \{2, 3\}$, with boundary decomposition $\partial\Omega = \Gamma_D \cup \Gamma_N$, where $\Gamma_D \cap \Gamma_N = \emptyset$, described by

Extended author information available on the last page of the article

Published online: 16 April 2026

$$\begin{aligned} (\boldsymbol{u}\cdot\nabla)T-\Delta T &= 0 \text{ in } \Omega,\\ T &= T_D \text{ on } \Gamma_D,\\ \nabla T\cdot \mathrm{n} &= 0 \text{ on } \Gamma_N,\\ -\mathrm{Pr}\Delta\boldsymbol{u}+(\boldsymbol{u}\cdot\nabla)\boldsymbol{u}+\nabla p &= \mathrm{PrRa}T\,\mathrm{g} \text{ in } \Omega,\\ \nabla\cdot\boldsymbol{u} &= 0 \text{ in } \Omega,\\ \boldsymbol{u} &= 0 \text{ in } \partial\Omega, \end{aligned} \tag{1.1}$$

where $(\boldsymbol{u}, p, T)$ denote the velocity, pressure, and temperature fields, respectively. The outward unit normal vector to Ω is denoted by n, and g represents the unit gravitational direction. The Prandtl and Rayleigh numbers are denoted by Pr and Ra, respectively. Finally, $T_D \in H^{1/2}(\Gamma_D)$ denotes the prescribed temperature on the Dirichlet portion of the boundary Γ_D.

The need to solve (1.1) arises in a wide range of scientific and engineering applications, including general atmospheric circulation [24], oceanic flows [21], heat pipes and heat exchangers [4], thermal energy storage systems, chemical reactors, and industrial cooling processes. Given the central role of these models in such applications, the development of accurate and efficient numerical techniques for approximating the resulting coupled partial differential equations remains of fundamental importance.

There has been significant interest in the development and analysis of efficient numerical methods for the Boussinesq equations, with notable contributions from various researchers [9, 13, 14, 22, 28, 32, 34]. In particular, the Boussinesq system (1.1) is frequently employed to model high–Rayleigh number natural convection problems [31], where continuation strategies are often required to ensure convergence.

One of the earliest finite element studies of (1.1) was carried out by Boland and Layton [3]. More recent advances include the mixed finite element formulations in [7, 27]. In [27], the authors proposed a mixed finite element method featuring exactly divergence-free velocities for a generalized Boussinesq system. Neilan et al. [7] introduced two mixed formulations incorporating the velocity gradient and Bernoulli stress tensor as auxiliary variables, establishing well-posedness and optimal error estimates for the corresponding finite element approximations.

Another prominent strategy for solving such saddle-point problems is the classical Arrow–Hurwicz (AH) iterative method [1]. One of the earliest applications in computational fluid dynamics appears in [35], where a Galerkin finite element formulation of the steady-state Navier–Stokes equations was studied. Interest in the AH method has recently been renewed following the work of [5], which established contractivity under suitable assumptions on the data and model parameters. Since then, a growing body of literature has explored AH-based solvers for the stationary Navier–Stokes equations. For example, the incorporation of grad-div stabilization and Anderson acceleration has been shown to enhance convergence [10]. Nonetheless, as demonstrated in [12], the classical AH method may fail to converge for certain parameter regimes when applied to general saddle-point systems. Motivated by the success of [5], AH-type approaches have also been developed for stationary magnetohydrodynamics (MHD) [37] and thermally coupled MHD systems [15].

A recent advancement in this direction is the improved Arrow–Hurwicz (AH) method introduced in [33], derived from a first-order time discretization of an artifi-

cial compressibility formulation for the steady-state Navier–Stokes equations. This approach has also been successfully extended to the steady-state Smagorinsky model in [16]. As demonstrated in [33], the improved AH method maintains stronger theoretical foundations than the classical formulation of [5] and significantly accelerates convergence to the steady state.

Motivated by the work of [33], we propose an Improved Arrow–Hurwicz (IAH) method for the steady-state Boussinesq system (1.1). A direct Arrow–Hurwicz (AH) formulation could, in principle, be applied solely to the momentum equation, leading to the alternative scheme summarized in Algorithm 4.1. However, although this approach is consistent with the classical AH framework, we find that incorporating an AH-type update for the temperature terms in the energy equation (2.5) is essential. In particular, this modification is necessary to ensure enhanced computational efficiency and robust convergence, especially at high Rayleigh numbers. We therefore refer to Algorithm 4.1 as the alternative Arrow–Hurwicz (AAH) method, while Algorithm 3.1 defines the proposed Improved Arrow–Hurwicz (IAH) variant. We provide a complete numerical analysis of the IAH method under reasonable small-data conditions for (1.1), and present extensive computational experiments demonstrating its accuracy, efficiency, and superior convergence properties—even in parameter regimes where the AAH method fails.

The main contributions of this work are

- Extension of the improved Arrow–Hurwicz framework to the steady-state Boussinesq equations with nonhomogeneous temperature boundary conditions.
- Design of an AH-type update for the energy equation, which is shown to be essential for robust convergence, particularly at high Rayleigh numbers.
- Rigorous mathematical analysis, establishing existence, uniqueness, uniform boundedness, and error estimates under standard small-data conditions.
- Extensive two- and three-dimensional numerical experiments demonstrating accuracy, robustness, and superior convergence relative to both the alternative AH scheme and the classical Penalty–Picard Iteration (PPI).

The structure of the paper is as follows. Section 2 introduces the notation and presents preliminary results, including the a priori estimates of both the continuous problem and its finite element discretization. Section 3 is devoted to the analysis of the proposed IAH scheme, where we establish the uniform boundedness and uniqueness of the finite element solutions and derive corresponding error estimates. Numerical experiments in two and three dimensions are reported in Sect. 4, and concluding remarks are given in Sect. 5.

2 Preliminaries

The standard notations will be used for Lebesgue and Sobolev spaces. The L^2 norm and inner product are denoted by $\|\cdot\|$ and $(\cdot,\cdot)$. As usual, the velocity and pressure spaces are denoted by $\mathrm{X} = \left(H_0^1(\Omega)\right)^d$ and $Q = L_0^2(\Omega)$, and the divergence-free

space and the temperature space are denoted by V and $W := H_0^1(\Omega)$, respectively. We note that the spaces X and W are equipped with the norms $\|\mathrm{v}\|_{\mathrm{X}} = \|\nabla \mathrm{v}\|$ and $\|S\|_W = \|\nabla S\|$, respectively. In addition, we let $H^{1/2}(\Gamma_D)$ be the trace space obtained as the image of $H^1(\Omega)$ on the boundary value of Γ_D.

For all $\boldsymbol{u}, \mathrm{v}, \mathrm{w} \in X$, and $T, S \in W$, define two usual trilinear forms

$$b_1(\boldsymbol{u}, T, S) := ((\boldsymbol{u} \cdot \nabla)T, S) + \frac{1}{2}(\nabla \cdot \boldsymbol{u}, S\,T), \tag{2.1}$$

$$b_2(\boldsymbol{u}, \mathrm{v}, \mathrm{w}) := ((\boldsymbol{u} \cdot \nabla)\mathrm{v}, \mathrm{w}) + \frac{1}{2}(\nabla \cdot \boldsymbol{u}, \mathrm{v} \cdot \mathrm{w}), \tag{2.2}$$

satisfying the bounds

$$b_1(\boldsymbol{u}, T, S) \le \mathcal{M}_1 \|\nabla \boldsymbol{u}\| \|\nabla T\| \|\nabla S\|, \tag{2.3}$$

$$b_2(\boldsymbol{u}, \mathrm{v}, \mathrm{w}) \le \mathcal{M}_2 \|\nabla \boldsymbol{u}\| \|\nabla \mathrm{v}\| \|\nabla \mathrm{w}\|, \tag{2.4}$$

where $\mathcal{M}_1 = \mathcal{M}_1(\Omega), \mathcal{M}_2 = \mathcal{M}_2(\Omega)$ are positive constants. The proofs of the inequalities (2.3)-(2.4) can be found in [11].

It is observed that for all $\boldsymbol{u}, \mathrm{v}, \mathrm{w} \in X$, and $T, S \in W$, the trilinear forms (2.1) and (2.2) satisfy

$$b_1(\boldsymbol{u}, T, S) = -b_1(\boldsymbol{u}, S, T), \quad b_2(\boldsymbol{u}, \mathrm{v}, \mathrm{w}) = -b_2(\boldsymbol{u}, \mathrm{w}, \mathrm{v}), \quad b_1(\boldsymbol{u}, S, S) = 0, \quad b_2(\boldsymbol{u}, \mathrm{v}, \mathrm{v}) = 0.$$

We frequently use the Poincaré inequality for all $\mathrm{v} \in \mathrm{X}$

$$\|\mathrm{v}\| \le C_p \|\nabla \mathrm{v}\|,$$

where $C_p = C_p(\Omega)$.

2.1 Reformulation of the problem

We first decompose the temperature as $T = \theta + \widetilde{T}$, where $\widetilde{T} = E_\delta T_D \in H^1(\Omega)$ is an extension of the Dirichlet data T_D described in Lemma 2.1 below; then by using new variable $\theta = T - \widetilde{T} \in W$, (1.1) is transformed into

$$\begin{aligned}
(\boldsymbol{u} \cdot \nabla)(\theta + \widetilde{T}) - \Delta(\theta + \widetilde{T}) &= 0 \text{ in } \Omega, \\
\theta &= 0 \text{ on } \Gamma_D, \\
\nabla(\theta + \widetilde{T}) \cdot \mathrm{n} &= 0 \text{ on } \Gamma_N, \\
-\mathrm{Pr}\Delta \boldsymbol{u} + (\boldsymbol{u} \cdot \nabla)\boldsymbol{u} + \nabla p &= \mathrm{Pr}\,\mathrm{Ra}\,(\theta + \widetilde{T})\,\mathrm{g} \text{ in } \Omega, \\
\nabla \cdot \boldsymbol{u} &= 0 \text{ in } \Omega, \\
\boldsymbol{u} &= 0 \text{ on } \partial\Omega.
\end{aligned} \tag{2.5}$$

The weak formulation of the resulting system of equations (2.5) is then given by: Find $(\boldsymbol{u}, p, \theta) \in (\mathrm{X}, Q, W)$ satisfying

$$(\nabla\theta, \nabla S) + b_1(\boldsymbol{u}, \theta, S) = -b_1(\boldsymbol{u}, \widetilde{T}, S) - (\nabla\widetilde{T}, \nabla S), \tag{2.6}$$

$$\mathrm{Pr}(\nabla\boldsymbol{u}, \nabla\mathrm{v}) + b_2(\boldsymbol{u}, \boldsymbol{u}, \mathrm{v}) = (p, \nabla\cdot\mathrm{v}) + \mathrm{Pr}\,\mathrm{Ra}d(\theta, \mathrm{v}) + \mathrm{Pr}\,\mathrm{Ra}\,d(\widetilde{T}, \mathrm{v}), \tag{2.7}$$

$$(\nabla\cdot\boldsymbol{u}, q) = 0, \tag{2.8}$$

for all $(v, q, S) \in (\mathrm{X}, Q, W)$, where $d(T, \mathrm{v}) := (T\mathrm{g}, \mathrm{v})$.

2.2 Existence and uniqueness results

We now state some important results concerning the existence and uniqueness of (2.6)-(2.8). Firstly, we recall that for every $T_D \in H^{1/2}(\Gamma_D)$, the equations (2.6)-(2.8) have a solution, e.g., see [18, 26].

Next, we recall a Lemma about lifting of the boundary data T_D, adapted from [7, Lemma 3.2].

Lemma 2.1 *Let $\Omega \subset R^d$, $d = 2, 3$, be a bounded domain with Lipschitz continuous boundary. Then $\forall\delta > 0$ there exists an extension operator $E_\delta : H^{1/2}(\Gamma_D) \to H^1(\Omega)$ such that*

$$\|E_\delta T_D\|_3 \le C\delta\|T_D\|_{1/2,\Gamma_D} and \|\nabla E_\delta T_D\| \le C\delta^{-4}\|T_D\|_{1/2,\Gamma_D}.$$

Next, we derive a priori bounds for the solution of (2.5):

Lemma 2.2 *Assume $(\boldsymbol{u}, \theta)$ is a solution of (2.6)-(2.8). Then there exist $C_1 > 0$ and $C_2 > 0$ such that the following inequalities hold:*

$$\|\nabla\boldsymbol{u}\| \le C_1\mathrm{Ra}^5\|T_D\|^5_{1/2,\Gamma_D} =: C_u, \tag{2.9}$$

$$\|\nabla\theta\| \le C_2\mathrm{Ra}^4\|T_D\|^5_{1/2,\Gamma_D} =: C_\theta. \tag{2.10}$$

Proof Choose $S = \theta$ in (2.6), then by Lemma 2.1 and Sobolev embedding theorems, $\forall\delta > 0$ we have that

$$\begin{aligned} -b_1(\boldsymbol{u}, \widetilde{T}, \theta) &= b_1(\boldsymbol{u}, \theta, \widetilde{T}) \\ &\le \|\boldsymbol{u}\|_6\|\nabla\theta\|\|\widetilde{T}\|_3 \\ &\le C_3\delta\|\nabla\boldsymbol{u}\|\|\nabla\theta\|\|T_D\|_{1/2,\Gamma_D}. \end{aligned} \tag{2.11}$$

Then using (2.11), $b_1(\boldsymbol{u}, \theta, \theta) = 0$ and the Cauchy-Schwarz inequality we obtain

$$\|\nabla\theta\| \leq C_4 \left(\delta\|\nabla \boldsymbol{u}\| + \delta^{-4}\right) \|T_D\|_{1/2,\Gamma_D}. \tag{2.12}$$

Next setting $\mathrm{v} = \boldsymbol{u}$, $q = p$ in (2.7) and (2.8) yields

$$\|\nabla \boldsymbol{u}\| \leq C_5 \mathrm{Ra} \left(\|\nabla\theta\| + \delta^{-4}\|T_D\|_{1/2,\Gamma_D}\right), \tag{2.13}$$

for some appropriate $C_5 > 0$. Combining (2.12) and (2.13) produces

$$\left(1 - C_6 \mathrm{Ra}\, \delta \|T_D\|_{1/2,\Gamma_D}\right) \|\nabla \boldsymbol{u}\| \leq C_6 \mathrm{Ra}\, \delta^{-4} \|T_D\|_{1/2,\Gamma_D}. \tag{2.14}$$

Finally, choosing

$$\delta = \frac{1}{2C_6 \mathrm{Ra} \|T_D\|_{1/2,\Gamma_D}} \tag{2.15}$$

completes the proof. □

Theorem 2.1 *(Uniqueness) Let*

$$\tilde{\Lambda} := \mathrm{Pr} - \mathrm{Pr}\,\mathrm{Ra} C_p^2 \mathcal{M}_1 \tilde{C}_T - \mathcal{M}_2 \tilde{C}_u > 0. \tag{2.16}$$

Then $(\boldsymbol{u}, p, \theta)$ *is the unique solution of (2.6)-(2.8).*

Proof Assume $(\boldsymbol{u}_i, \theta_i) \in (\mathrm{V}, W)$, $i = 1, 2$, are two solutions of (2.6) and (2.7). Setting $\boldsymbol{\varepsilon_u} = \boldsymbol{u}_1 - \boldsymbol{u}_2$ and $\varepsilon_\theta = \theta_1 - \theta_2$, subtracting them results in

$$(\nabla \varepsilon_\theta, \nabla S) + b_1(\boldsymbol{\varepsilon_u}, \theta_1, S) + b_1(\boldsymbol{u}_2, \varepsilon_\theta, S) = -b_1(\boldsymbol{\varepsilon_u}, \widetilde{T}, S), \tag{2.17}$$

$$\mathrm{Pr}(\nabla \boldsymbol{\varepsilon_u}, \nabla \mathrm{v}) + b_2(\boldsymbol{\varepsilon_u}, \boldsymbol{u}_1, \mathrm{v}) + b_2(\boldsymbol{u}_2, \boldsymbol{\varepsilon_u}, \mathrm{v}) = \mathrm{Pr}\,\mathrm{Ra}\, d(\varepsilon_\theta, \mathrm{v}). \tag{2.18}$$

Letting $(\mathrm{v}, S) = (\boldsymbol{\varepsilon_u}, \varepsilon_\theta)$ in (2.17)-(2.18), and applying the skew-symmetry of nonlinear terms produces

$$\begin{aligned} \|\nabla \varepsilon_\theta\|^2 &= -b_1(\boldsymbol{\varepsilon_u}, \theta_1 + \widetilde{T}, \varepsilon_\theta), \\ \mathrm{Pr}\|\nabla \boldsymbol{\varepsilon_u}\|^2 &= \mathrm{Pr}\,\mathrm{Ra}\, d(\varepsilon_\theta, \boldsymbol{\varepsilon_u}) - b_2(\boldsymbol{\varepsilon_u}, \boldsymbol{u}_1, \boldsymbol{\varepsilon_u}). \end{aligned}$$

Using (2.3)-(2.4), and Lemma 2.2, we get

$$\begin{aligned} &\|\nabla \varepsilon_\theta\| \leq \mathcal{M}_1 \tilde{C}_T \|\nabla \boldsymbol{\varepsilon_u}\| \Longrightarrow \\ &\mathrm{Pr}\|\nabla \boldsymbol{\varepsilon_u}\|^2 \leq \mathrm{Pr}\,\mathrm{Ra} C_p^2 \mathcal{M}_1 \tilde{C}_T \|\nabla \boldsymbol{\varepsilon_u}\|^2 + \mathcal{M}_2 \tilde{C}_u \|\nabla \boldsymbol{\varepsilon_u}\|^2, \end{aligned}$$

where $\tilde{C}_T = C_2 \mathrm{Ra}^4 \|T_D\|^5_{1/2,\Gamma_D}$ and $\tilde{C}_u = C_1 \mathrm{Ra}^5 \|T_D\|^5_{1/2,\Gamma_D}$. Thanks to (2.16), we have that $\boldsymbol{\varepsilon_u} = 0$ and $\varepsilon_\theta = 0$. The uniqueness of p then is obtained from the inf-sup condition. □

Remark 2.1 *Assumptions like the "small data condition" (2.16) will come up often in the study of steady problems. Computing the exact value of $\tilde{\Lambda}$ is extremely technical and beyond practical. However, in this case, it can be interpreted as imposing a small value of* Ra. *That is because often* $\mathrm{Pr} = \mathcal{O}(1)$, *and Lemma 2.2 implies that upbounding constants* C_u, C_θ, *etc., are all* $\simeq \mathcal{O}(\mathrm{Ra}^k), k > 0$.

2.3 Finite element formulation

Let $\mathcal{T}_h$ be a regular triangulation of the domain Ω with maximum diameter length h. We will assume that for an element K, if $K \cap \Gamma_D \neq \emptyset$, then $K \cap \Gamma_N = \emptyset$. Assume that X_h, Q_h and W_h are the finite element subspaces of X, Q and W, respectively. The discretely divergence-free space is denoted by V_h. Also, suppose that (X_h, Q_h) satisfy usual inf-sup condition:

$$\inf_{q_h \in Q_h} \sup_{\mathrm{v}_h \in \mathrm{X}_h} \frac{(q_h, \nabla \cdot \mathrm{v}_h)}{\|\nabla \mathrm{v}_h\| \|q_h\|} \geq \beta = \beta(\Omega) > 0. \tag{2.19}$$

Next, we define the finite element approximation of the Dirichlet data T_D following [7]. To this end, let

$$\mathrm{SZ}_h : H^1(\Omega) \to W_h$$

be the Scott-Zhang interpolating operator [30]. Recalling the $E_\delta T_D$ extension operator from Lemma 2.1, we define the finite element approximation of Dirichlet data as

$$\widetilde{T}_h := \mathrm{SZ}_h(E_\delta T_D) \text{ and } T_{D,h} := \widetilde{T}_h\Big|_{\Gamma_D}. \tag{2.20}$$

Then Galerkin finite element approximation of equation (2.6)-(2.8) takes the following form: for all $(\mathrm{v}_h, q_h, S_h) \in (\mathrm{X}_h, Q_h, W_h)$, find $(\boldsymbol{u}_h, p_h, \theta_h) \in (\mathrm{X}_h, Q_h, W_h)$ satisfying

$$(\nabla \theta_h, \nabla S_h) + b_1(\boldsymbol{u}_h, \theta_h, S_h) = -b_1(\boldsymbol{u}_h, \widetilde{T}_h, S_h) - (\nabla \widetilde{T}_h, \nabla S_h), \tag{2.21}$$

$$\mathrm{Pr}(\nabla \boldsymbol{u}_h, \nabla \mathrm{v}_h) + b_2(\boldsymbol{u}_h, \boldsymbol{u}_h, \mathrm{v}_h) = (p_h, \nabla \cdot \mathrm{v}_h) + \mathrm{Pr}\,\mathrm{Ra}\, d(\theta_h, \mathrm{v}_h) + \mathrm{Pr}\,\mathrm{Ra}\, d(\widetilde{T}_h, \mathrm{v}_h), \tag{2.22}$$

$$(\nabla \cdot \boldsymbol{u}_h, q_h) = 0. \tag{2.23}$$

Properties of discrete extension $\widetilde{T}_h$ are given in [7, Lemma 4.3]:

Lemma 2.3 *For any $\delta > 0$, there exists $h_\delta > 0$ such that, for $h \leq h_\delta$ there holds*

$$\|\widetilde{T}_h\|_3 \leq C\delta \|T_D\|_{1/2,\Gamma_D} \text{and} \|\nabla \widetilde{T}_h\| \leq C\delta^{-4} \|T_D\|_{1/2,\Gamma_D}. \tag{2.24}$$

Assuming that $\delta = \mathcal{O}(\mathrm{Ra}^{-1})$, the last Lemma requires that the diameter of mesh h to be taken as $h = \mathcal{O}(\mathrm{Ra}^{-30/(6-d)})$ [7, Lemma 4.3], where d is a space dimension.

Recalling the quasi-locality of the Scott-Zhang interpolant, the above assumption can be relaxed to $h_D = \mathcal{O}(\mathrm{Ra}^{-30/(6-d)})$, where h_D is the diameter of the elements either adjacent to Γ_D or within a small distance of Γ_D.

Remark 2.2 *The mesh size condition $h_D = \mathcal{O}\left(\mathrm{Ra}^{-\frac{30}{6-d}}\right)$ is standard in the theoretical analysis of such systems, see also [9]. In practice, however, our computations exhibit little sensitivity to this assumption; see Sect. 4.*

Lemma 2.4 *Assume $(\boldsymbol{u}_h, p_h, \theta_h)$ is a solution of (2.21)-(2.23) and $h_D = \mathcal{O}(\mathrm{Ra}^{-1})$. Then there exist constants $C_u > 0$, $C_p > 0$, $C_\theta > 0$ and $C_T > 0$ such that the following inequalities hold:*

$$\|\nabla \boldsymbol{u}_h\| \leq C_u, \ \|p_h\| \leq C_p, \ \|\nabla \theta_h\| \leq C_\theta, and \|\theta_h + \widetilde{T}_h\| \leq C_T. \tag{2.25}$$

Proof The proof closely follows the arguments of Lemma 2.2. □

Remark 2.3 *The existence result for the discrete problem (2.21)-(2.23) is established using the same arguments as in the continuous case presented in [7, Theorem 4.7].*

Furthermore, we have the uniqueness result:

Theorem 2.2 *(Uniqueness) Let*

$$\Lambda := \mathrm{Pr} - \mathrm{Pr}\,\mathrm{Ra} C_p^2 \mathcal{M}_1 C_T - \mathcal{M}_2 C_u > 0. \tag{2.26}$$

Then $(\boldsymbol{u}_h, p_h, \theta_h)$ is the unique solution of (2.21)-(2.23).

Proof Suppose $(\boldsymbol{u}_{i,h}, \theta_{i,h}) \in (\mathrm{V}_h, W_h)$, $i = 1, 2$, are the two distinct solutions of (2.21)-(2.23). Letting $\boldsymbol{\varepsilon}_{\boldsymbol{u},h} = \boldsymbol{u}_{1,h} - \boldsymbol{u}_{2,h}$ and $\varepsilon_{\theta,h} = \theta_{1,h} - \theta_{2,h}$, subtracting them yields

$$(\nabla \varepsilon_{\theta,h}, \nabla S_h) + b_1(\boldsymbol{u}_{1,h}, \theta_{1,h}, S_h) - b_1(\boldsymbol{u}_{2,h}, \theta_{2,h}, S_h) = -b_1(\boldsymbol{\varepsilon}_{\boldsymbol{u},h}, \widetilde{T}_h, S_h), \tag{2.27}$$

$$\mathrm{Pr}(\nabla \boldsymbol{\varepsilon}_{\boldsymbol{u},h}, \nabla \mathrm{v}_h) + b_2(\boldsymbol{u}_{1,h}, \boldsymbol{u}_{1,h}, \mathrm{v}_h) - b_2(\boldsymbol{u}_{2,h}, \boldsymbol{u}_{2,h}, \mathrm{v}_h) = \mathrm{Pr}\,\mathrm{Ra}\, d(\varepsilon_{\theta,h}, \mathrm{v}_h). \tag{2.28}$$

Choosing $\mathrm{v}_h = \boldsymbol{\varepsilon}_{\boldsymbol{u},h}$ and $S_h = \varepsilon_{\theta,h}$ above, and using the skew-symmetry properties, one has

$$\|\nabla \varepsilon_{\theta,h}\|^2 = -b_1(\boldsymbol{\varepsilon}_{\boldsymbol{u},h}, \theta_{1,h} + \widetilde{T}_h, \varepsilon_{\theta,h}), \tag{2.29}$$

$$\mathrm{Pr}\|\nabla \boldsymbol{\varepsilon}_{\boldsymbol{u},h}\|^2 = \mathrm{Pr}\,\mathrm{Ra}\, d(\varepsilon_{\theta,h}, \boldsymbol{\varepsilon}_{\boldsymbol{u},h}) - b_2(\boldsymbol{\varepsilon}_{\boldsymbol{u},h}, \boldsymbol{u}_{1,h}, \boldsymbol{\varepsilon}_{\boldsymbol{u},h}). \tag{2.30}$$

Then (2.29) immediately yields

$$\|\nabla\varepsilon_{\theta,h}\| \leq \mathcal{M}_1 C_T \|\nabla\boldsymbol{\varepsilon}_{\boldsymbol{u},h}\|. \tag{2.31}$$

Utilizing (2.31) in (2.30) gives

$$\Pr\|\nabla\boldsymbol{\varepsilon}_{\boldsymbol{u},h}\|^2 \leq \Pr \mathrm{Ra} C_p^2 \mathcal{M}_1 C_T \|\nabla\boldsymbol{\varepsilon}_{\boldsymbol{u},h}\|^2 + \mathcal{M}_2 C_u \|\nabla\boldsymbol{\varepsilon}_{\boldsymbol{u},h}\|^2. \tag{2.32}$$

In light of (2.26), the inequality (2.32) is equivalent to

$$\Lambda\|\nabla\boldsymbol{\varepsilon}_{\boldsymbol{u},h}\|^2 < 0, \tag{2.33}$$

which implies that $\boldsymbol{\varepsilon}_{\boldsymbol{u},h} = 0$. Then (2.31) gives $\varepsilon_{\theta,h} = 0$, and by the inf-sup condition, we also get the uniqueness of p_h. □

3 Improved AH method

This section presents the proposed improved AH method Algorithm 3.1 and proofs of uniform boundedness and convergence results.

Algorithm 3.1. *Improved Arrow–Hurwicz Method (IAH): Let ρ_u, ρ_T, and α be positive parameters, and initialize $(\mathbf{u}_h^0, p_h^0, \theta_h^0) = (\mathbf{0}, 0, 0)$. For $n \geq 0$, find $(\mathbf{u}_h^{n+1}, p_h^{n+1}, \theta_h^{n+1}) \in (\mathbf{X}_h, Q_h, W_h)$ such that, for all $(\mathbf{v}_h, q_h, S_h) \in (\mathbf{X}_h, Q_h, W_h)$,*

$$\frac{1}{\rho_T}(\nabla(\theta_h^{n+1} - \theta_h^n), \nabla S_h) + b_1(\mathbf{u}_h^n, \theta_h^{n+1}, S_h) + (\nabla\theta_h^{n+1}, \nabla S_h) = -b_1(\mathbf{u}_h^n, \widetilde{T}_h, S_h) - (\nabla\widetilde{T}_h, \nabla S_h), \tag{3.1}$$

$$\frac{1}{\rho_u}(\nabla(\mathbf{u}_h^{n+1} - \mathbf{u}_h^n), \nabla\mathbf{v}_h) + \Pr(\nabla\mathbf{u}_h^{n+1}, \nabla\mathbf{v}_h) + b_2(\mathbf{u}_h^n, \mathbf{u}_h^{n+1}, \mathbf{v}_h) - (p_h^n, \nabla\cdot\mathbf{v}_h) + \frac{\rho_u}{\alpha}(\nabla\cdot\mathbf{u}_h^{n+1}, \nabla\cdot\mathbf{v}_h)$$
$$= \Pr \mathrm{Ra}\, d(\theta_h^{n+1}, \mathbf{v}_h) + \Pr \mathrm{Ra}\, d(\widetilde{T}_h, \mathbf{v}_h), \tag{3.2}$$

$$\alpha(p_h^{n+1} - p_h^n, q_h) + \rho_u(\nabla\cdot\mathbf{u}_h^{n+1}, q_h) = 0. \tag{3.3}$$

Remark 3.1 *A zero initial guess is adopted for simplicity; however, any initialization satisfying $\nabla\cdot\boldsymbol{u}_h^0 = 0$ may be used.*

First, we establish the well-posedness of the Algorithm 3.1.

Theorem 3.1 *(Existence and Uniqueness) For any $\rho_T > 0$, $\rho_u > 0$, $\alpha > 0$, the Algorithm 3.1 has a unique solution.*

Proof Since (3.1)-(3.3) is a finite-dimensional, linear system of equations, it suffices to show the uniqueness of the solution. To this end, we proceed by induction. Assuming that $\exists!\,(\boldsymbol{u}_h^n, p_h^n, \theta_h^n)$, we shall demonstrate the uniqueness of $(\boldsymbol{u}_h^{n+1}, p_h^{n+1}, \theta_h^{n+1})$.

Suppose that $(\boldsymbol{u}_{i,h}^{n+1}, p_{i,h}^{n+1}, \theta_{i,h}^{n+1})$, $i = 1, 2$, solve (3.1)-(3.3). Denoting their differences as

$$\epsilon_h^{n+1} := \theta_{1,h}^{n+1} - \theta_{2,h}^{n+1},\ \mathrm{e}_h^{n+1} := \boldsymbol{u}_{1,h}^{n+1} - \boldsymbol{u}_{2,h}^{n+1},\ \delta_h^{n+1} := p_{1,h}^{n+1} - p_{2,h}^{n+1},$$

we obtain the following system for them:

$$\frac{1}{\rho_T}(\nabla \epsilon_h^{n+1}, \nabla S_h) + b_1(\boldsymbol{u}_h^n, \epsilon_h^{n+1}, S_h) + (\nabla \epsilon_h^{n+1}, \nabla S_h) = 0, \tag{3.1}$$

$$\frac{1}{\rho_u}(\nabla \mathrm{e}_h^{n+1}, \nabla \mathrm{v}_h) + \mathrm{Pr}(\nabla \mathrm{e}_h^{n+1}, \nabla \mathrm{v}_h) + b_2(\boldsymbol{u}_h^n, \mathrm{e}_h^{n+1}, \mathrm{v}_h) + \frac{\rho_u}{\alpha}(\nabla \cdot \mathrm{e}_h^{n+1}, \nabla \cdot \mathrm{v}_h) = \mathrm{Pr}\,\mathrm{Ra}\, d(\epsilon_h^{n+1}, \mathrm{v}_h), \tag{3.2}$$

$$\alpha(\delta_h^{n+1}, q_h) + \rho_u(\nabla \cdot \mathrm{e}_h^{n+1}, q_h) = 0. \tag{3.3}$$

Now let $S_h = \epsilon_h^{n+1}$ in (3.4), to see that $\epsilon_h^{n+1} = 0$. Then picking $\mathrm{v}_h = \mathrm{e}_h^{n+1}$ in (3.5) implies that $\mathrm{e}_h^{n+1} = 0$, and choosing $q_h = \delta_h^{n+1}$ in (3.6) yields that $\delta_h^{n+1} = 0$. □

Next, we state two preliminary lemmas about non-negative sequences that will be used in the sequel, inspired from [8].

Lemma 3.1 *(Sequences converging to 0) If $\{a_n\}_{n=1}^{\infty}, \{b_n\}_{n=1}^{\infty}, \{c_n\}_{n=1}^{\infty}$ are non-negative sequences of real numbers and $\exists\, \omega_i,\ \varepsilon_i,\ i = 1, 2$, such that $0 < \varepsilon_i < \omega_i$ and*

$$\omega_1 a_{n+1} + \omega_2 b_{n+1} + c_{n+1} \leq (\omega_1 - \varepsilon_1)\, a_n + (\omega_2 - \varepsilon_2)\, b_n + c_n.$$

Then $\exists\, C \geq 0$ such that

$$\lim_{n\to\infty} (a_n, b_n, c_n) = (0, 0, C).$$

Proof Let $\phi_n := \omega_1 a_n + \omega_2 b_n + c_n$ and $\psi_n := (\omega_1 - \varepsilon_1)\, a_n + (\omega_2 - \varepsilon_2)\, b_n + c_n$. Then

$$\psi_{n+1} \leq \phi_{n+1} \leq \psi_n \leq \phi_n \Longrightarrow \lim_{n\to\infty} \phi_n = \lim_{n\to\infty} \psi_n = C \geq 0.$$

and

$$\phi_n - \psi_n = \varepsilon_1 a_n + \varepsilon_2 b_n \Longrightarrow \lim_{n\to\infty} a_n = \lim_{n\to\infty} b_n = 0 \text{ and } \lim_{n\to\infty} c_n = C.$$

□

Lemma 3.2 *(Contractivity of sequences converging to 0)*

If $\{a_n\}_{n=1}^{\infty}, \{b_n\}_{n=1}^{\infty}, \{c_n\}_{n=1}^{\infty}$ are non-negative sequences of real numbers and $\exists\, \omega_i,\ i = 1, 3,\ \varepsilon_i,\ i = 1, 2$, such that $0 < \varepsilon_i < \omega_i,\ i = 1, 2,$

$$\omega_1 a_{n+1} + \omega_2 b_{n+1} + \omega_3 c_{n+1} \leq (\omega_1 - \varepsilon_1)\, a_n + (\omega_2 - \varepsilon_2)\, b_n + \omega_3 c_n \tag{3.4}$$

and

$$c_n \leq \alpha a_{n+1} + \beta a_n + \gamma b_{n+1} for some positive \alpha, \beta, \gamma. \tag{3.5}$$

Then there exists a sequence, which is a linear combination of a_n, b_n, c_n that is contracting towards 0.

Proof For any $\xi > 0$, combine (3.7) and (3.8) to get

$$\begin{aligned}(\omega_1 - \alpha\xi)a_{n+1} + (\omega_2 - \gamma\xi)b_{n+1} + \omega_3 c_{n+1} \\ \leq (\omega_1 - \varepsilon_1 + \beta\xi)\, a_n + (\omega_2 - \varepsilon_2)\, b_n + (\omega_3 - \xi)\, c_n.\end{aligned} \tag{3.6}$$

For now, we require that

$$\xi < \min\left\{\frac{\omega_1}{\alpha}, \frac{\omega_2}{\gamma}, \omega_3\right\}.$$

Next, we additionally assume that

$$\frac{\omega_2 - \varepsilon_2}{\omega_2 - \gamma\xi} < \frac{\omega_3 - \xi}{\omega_3} \Longleftrightarrow f(\xi) := \gamma\xi^2 - \xi\,(\omega_2 + \gamma\omega_3) + \omega_3\varepsilon_2 > 0. \tag{3.7}$$

Note that, since $\varepsilon_2 < \omega_2$, the discriminant of $f(\xi) = 0$ is non-negative:

$$D = (\omega_2 + \gamma\omega_3)^2 - 4\gamma\omega_3\varepsilon_2 = \omega_2^2 + 2\gamma\omega_2\omega_3 + \gamma^2\omega_3^2 - 4\gamma\omega_3\varepsilon_2 \geq (\omega_2 - \gamma\omega_3)^2.$$

Thus, $f(\xi) = 0$ has two positive roots $0 < \xi_1 < \widehat{\xi}_1$. Therefore, choosing ξ such that

$$\xi < \min\left\{\frac{\omega_1}{\alpha}, \frac{\omega_2}{\gamma}, \omega_3, \xi_1\right\}$$

implies that (3.10) holds and

$$(\omega_1 - \alpha\xi)a_{n+1} + (\omega_2 - \gamma\xi)b_{n+1} + \omega_3 c_{n+1} \tag{3.8}$$

$$\leq (\omega_1 - \varepsilon_1 + \beta\xi)\, a_n + \frac{\omega_3 - \xi}{\omega_3}\left[(\omega_2 - \gamma\xi)\, b_n + \omega_3 c_n\right]. \tag{3.9}$$

Finally, assume that for some $\xi > 0$ small enough there holds

$$\frac{\omega_1 - \varepsilon_1 + \beta\xi}{\omega_1 - \alpha\xi} < \frac{\omega_3 - \xi}{\omega_3} \Longleftrightarrow g(\xi) := \alpha\xi^2 - \xi(\omega_1 + \alpha\omega_3 + \beta\omega_3) + \omega_3\varepsilon_1 > 0. \tag{3.10}$$

Just like above, the discriminant of the equation $g(\xi) = 0$ is non-negative:

$$D = (\omega_1 + (\alpha+\beta)\omega_3)^2 - 4\alpha\omega_3\varepsilon_1 \geq (\omega_1 - (\alpha+\beta)\omega_3)^2 .$$

Now denote the two roots of $g(\xi) = 0$ as $0 < \xi_2 < \widehat{\xi}_2$. Then choosing ξ such that

$$\xi < \min\left\{\frac{\omega_1}{\alpha}, \frac{\omega_2}{\gamma}, \omega_3, \xi_1, \xi_2\right\}$$

ensures that

$$(\omega_1 - \alpha\xi)a_{n+1} + (\omega_2 - \gamma\xi)b_{n+1} + \omega_3 c_{n+1} \tag{3.11}$$

$$\leq \frac{\omega_3 - \xi}{\omega_3}\left[(\omega_1 - \alpha\xi)a_n + (\omega_2 - \gamma\xi)b_n + \omega_3 c_n\right]. \tag{3.12}$$

Then $\psi_n := (\omega_1 - \alpha\xi)a_n + (\omega_2 - \gamma\xi)b_n + \omega_3 c_n$ is a contracting sequence with a contraction factor $\kappa := \dfrac{\omega_3 - \xi}{\omega_3} < 1$. □

Theorem 3.2 *(Uniform boundedness) Assume that* $(\boldsymbol{u}_h, p_h, \theta_h) \in (\mathrm{X}_h, Q_h, W_h)$ *is a solution of (2.21)-(2.23) and* $\{\boldsymbol{u}_h^n, p_h^n, \theta_h^n\}$ *is the function sequence generated by (3.1)-(3.3). If*

$$\begin{aligned} \Lambda_1 := \mathrm{Pr} - \mathcal{M}_2 C_u - \frac{\mathrm{Pr}^2\,\mathrm{Ra}^2 C_p^4}{2} - \frac{{\mathcal{M}_1}^2 C_T^2}{2} > 0 and \rho_u < \frac{2\Lambda_1}{{\mathcal{M}_2}^2 C_u^2}, \\ and \Lambda_2 := \Lambda_1 - \rho_u \frac{{\mathcal{M}_2}^2 C_u^2}{2} > 0 and \rho_T < \frac{2\Lambda_2}{{\mathcal{M}_1}^2 C_T^2}, \end{aligned} \tag{3.13}$$

then $\{\boldsymbol{u}_h^n, p_h^n, \theta_h^n\}$ *is uniformly bounded and* $\boldsymbol{u}_h^n \xrightarrow{H^1} \boldsymbol{u}_h$ *as* $n \to \infty$.

Moreover, if

$$\begin{aligned} \widehat{\Lambda}_1 := \mathrm{Pr} - \mathcal{M}_2 C_u - \mathrm{Pr}^2\,\mathrm{Ra}^2 C_p^4 - \frac{{\mathcal{M}_1}^2 C_T^2}{2} > 0 and \rho_u < \frac{2\widehat{\Lambda}_1}{{\mathcal{M}_2}^2 C_u^2}, \\ and \widehat{\Lambda}_2 := \widehat{\Lambda}_1 - \rho_u \frac{{\mathcal{M}_2}^2 C_u^2}{2} > 0 and \rho_T < \frac{2\widehat{\Lambda}_2}{{\mathcal{M}_1}^2 C_T^2}, \end{aligned} \tag{3.14}$$

then $\boldsymbol{u}_h^n \xrightarrow{H^1} \boldsymbol{u}_h$, $p_h^n \xrightarrow{L^2} p_h and\, T_h^n \xrightarrow{H^1} T_h as n \to \infty$.

Proof Subtracting (3.1)-(3.3) from (2.21)-(2.23) we get the error equation:

$$\begin{aligned}&\frac{1}{\rho_T}(\nabla(\epsilon_h^{n+1}-\epsilon_h^n),\nabla S_h)+b_1(\mathrm{e}_h^n,\theta_h,S_h)\\&+b_1(\boldsymbol{u}_h^n,\epsilon_h^{n+1},S_h)+(\nabla\epsilon_h^{n+1},\nabla S_h)\\&=-b_1(\mathrm{e}_h^n,\widetilde{T}_h,S_h),\end{aligned}\tag{3.15}$$

$$\begin{aligned}&\frac{1}{\rho_u}(\nabla\mathrm{e}_h^{n+1}-\nabla\mathrm{e}_h^n,\nabla\mathrm{v}_h)+\mathrm{Pr}(\nabla\mathrm{e}_h^{n+1},\nabla\mathrm{v}_h)+b_2(\mathrm{e}_h^n,\boldsymbol{u}_h,\mathrm{v}_h)\\&\qquad+\frac{\rho_u}{\alpha}(\nabla\cdot\mathrm{e}_h^{n+1},\nabla\cdot\mathrm{v}_h)\quad+b_2(\boldsymbol{u}_h^n,\mathrm{e}_h^{n+1},\mathrm{v}_h)\\&\qquad-(\delta_h^n,\nabla\cdot\mathrm{v}_h)=\mathrm{Pr}\,\mathrm{Ra}\,d(\epsilon_h^{n+1},\mathrm{v}_h),\end{aligned}\tag{3.16}$$

$$\alpha(\delta_h^{n+1}-\delta_h^n,q_h)+\rho_u(\nabla\cdot\mathrm{e}_h^{n+1},q_h)=0,\tag{3.17}$$

where $\epsilon_h^n=\theta_h-\theta_h^n$, $\mathrm{e}_h^n=\boldsymbol{u}_h-\boldsymbol{u}_h^n$ and $\delta_h^n=p_h-p_h^n$. Choosing $S_h=\epsilon_h^{n+1}$, $\mathrm{v}_h=\mathrm{e}_h^{n+1}$ and $q_h=\delta_h^n$ in (3.16)-(3.18) and using $b_2(\boldsymbol{u}_h^n,\mathrm{e}_h^{n+1},\mathrm{e}_h^{n+1})=0$ and $b_1(\boldsymbol{u}_h^n,\epsilon_h^{n+1},\epsilon_h^{n+1})=0$, we have that

$$\frac{1}{2\rho_T}\Big(\|\nabla\epsilon_h^{n+1}\|^2-\|\nabla\epsilon_h^n\|^2+\|\nabla(\epsilon_h^{n+1}-\epsilon_h^n)\|^2\Big)+\|\nabla\mathrm{e}_h^{n+1}\|^2=-b_1(\mathrm{e}_h^n,\theta_h+\widetilde{T}_h,\epsilon_h^{n+1}),\tag{3.18}$$

$$\begin{aligned}&\frac{1}{2\rho_u}\Big(\|\nabla\mathrm{e}_h^{n+1}\|^2-\|\nabla\mathrm{e}_h^n\|^2+\|\nabla(\mathrm{e}_h^{n+1}-\mathrm{e}_h^n)\|^2\Big)+\mathrm{Pr}\|\nabla\mathrm{e}_h^{n+1}\|^2-(\delta_h^{n+1},\nabla\cdot\mathrm{e}_h^{n+1})\\&\qquad=-b_2\left(\mathrm{e}_h^n,\boldsymbol{u}_h,\mathrm{e}_h^{n+1}\right)+\mathrm{Pr}\,\mathrm{Ra}\,d(\epsilon_h^{n+1},\mathrm{e}_h^{n+1}),\end{aligned}\tag{3.19}$$

$$\frac{\alpha}{2\rho_u}(\|\delta_h^{n+1}\|^2-\|\delta_h^n\|^2-\|\delta_h^{n+1}-\delta_h^n\|^2)+(\nabla\cdot\mathrm{e}_h^{n+1},\delta_h^n)=0.\tag{3.20}$$

Choosing $q_h=\delta_h^{n+1}-\delta_h^n$ in (3.18) also implies that

$$\|\delta_h^{n+1}-\delta_h^n\|\le\frac{\rho_u}{\alpha}\|\nabla\cdot\mathrm{e}_h^{n+1}\|.\tag{3.21}$$

Combining (3.19)-(3.22), and dropping some nonnegative terms produces

$$\begin{aligned}&\frac{1}{2\rho_u}\Big(\|\nabla\mathrm{e}_h^{n+1}\|^2-\|\nabla\mathrm{e}_h^n\|^2+\|\nabla(\mathrm{e}_h^{n+1}-\mathrm{e}_h^n)\|^2\Big)+\mathrm{Pr}\|\nabla\mathrm{e}_h^{n+1}\|^2+\frac{\alpha}{2\rho_u}(\|\delta_h^{n+1}\|^2-\|\delta_h^n\|^2)\\&+\frac{1}{2\rho_T}\Big(\|\nabla\epsilon_h^{n+1}\|^2-\|\nabla\epsilon_h^n\|^2+\|\nabla(\epsilon_h^{n+1}-\epsilon_h^n)\|^2\Big)+\|\nabla\epsilon_h^{n+1}\|^2\\&\qquad\le|b_2(\mathrm{e}_h^n,\boldsymbol{u}_h,\mathrm{e}_h^{n+1})|+|b_1(\mathrm{e}_h^n,\theta_h+\widetilde{T}_h,\epsilon_h^{n+1})|+\mathrm{Pr}\,\mathrm{Ra}\,d(\epsilon_h^{n+1},\mathrm{e}_h^{n+1}).\end{aligned}\tag{3.22}$$

The right-hand side of the equation (3.23) can be bounded by (2.3), (2.4), (2.25) along with the Young's inequality:

$$\begin{aligned}|b_2(\mathrm{e}_h^n,\boldsymbol{u}_h,\mathrm{e}_h^{n+1})|\le&\mathcal{M}_2C_u\|\nabla\mathrm{e}_h^n\|\|\nabla\mathrm{e}_h^{n+1}\|\\\le&\mathcal{M}_2C_u\left(\|\nabla(\mathrm{e}_h^{n+1}-\mathrm{e}_h^n)\|+\|\nabla\mathrm{e}_h^{n+1}\|\right)\|\nabla\mathrm{e}_h^{n+1}\|\end{aligned}\tag{3.23}$$

$$
\begin{aligned}
&\leq \frac{1}{2\rho_u}\|\nabla(\mathrm{e}_h^{n+1}-\mathrm{e}_h^n)\|^2+\left(\mathcal{M}_2C_u+\frac{\rho_u{\mathcal{M}_2}^2C_u^2}{2}\right)\|\nabla\mathrm{e}_h^{n+1}\|^2,\\
|b_1(\mathrm{e}_h^n,\theta_h+\widetilde{T}_h,\epsilon_h^{n+1})| &\leq \mathcal{M}_1C_T\|\nabla\mathrm{e}_h^n\|\|\nabla\epsilon_h^{n+1}\|\\
&\leq \mathcal{M}_1C_T\left(\|\nabla(\epsilon_h^{n+1}-\epsilon_h^n)\|+\|\nabla\epsilon_h^n\|\right)\|\nabla\mathrm{e}_h^n\|
\end{aligned}
\tag{3.24}
$$

$$
\begin{aligned}
&\leq \frac{1}{2\rho_T}\|\nabla(\epsilon_h^{n+1}-\epsilon_h^n)\|^2+\frac{\rho_T+1}{2}{\mathcal{M}_1}^2C_T^2\|\nabla\mathrm{e}_h^n\|^2+\frac{1}{2}\|\nabla\epsilon_h^n\|^2,\\
\mathrm{Pr}\,\mathrm{Ra}\,d(\epsilon_h^{n+1},\mathrm{e}_h^{n+1}) &\leq \mathrm{Pr}\,\mathrm{Ra}C_p^2\|\nabla\epsilon_h^{n+1}\|\|\nabla\mathrm{e}_h^{n+1}\|\\
&\leq \frac{1}{2}\|\nabla\epsilon_h^{n+1}\|^2+\frac{\mathrm{Pr}^2\,\mathrm{Ra}^2C_p^4}{2}\|\nabla\mathrm{e}_h^{n+1}\|^2.
\end{aligned}
\tag{3.25}
$$

Substituting (3.24)-(3.26) into (3.23), using the definition of Λ_1 in (3.14), and dropping the non-negative terms gives

$$
\begin{aligned}
&\left(\frac{1}{2\rho_u}+\left[\Lambda_1-\rho_u\frac{{\mathcal{M}_2}^2C_u^2}{2}\right]+\frac{{\mathcal{M}_1}^2C_T^2}{2}\right)\|\nabla\mathrm{e}_h^{n+1}\|^2+\frac{\alpha}{2\rho_u}\|\delta_h^{n+1}\|^2+\frac{1+\rho_T^{-1}}{2}\|\nabla\epsilon_h^{n+1}\|^2\\
&\qquad\leq\left(\frac{1}{2\rho_u}+\frac{1+\rho_T}{2}{\mathcal{M}_1}^2C_T^2\right)\|\nabla\mathrm{e}_h^n\|^2+\frac{\alpha}{2\rho_u}\|\delta_h^n\|^2+\frac{1+\rho_T^{-1}}{2}\|\nabla\epsilon_h^n\|^2.
\end{aligned}
\tag{3.26}
$$

By assumption on ρ_u and ρ_T, we recall that

$$
\Lambda_2=\Lambda_1-\rho_u\frac{{\mathcal{M}_2}^2C_u^2}{2}>0,
$$

which allows us to define

$$
\Lambda_3:=\Lambda_2-\rho_T\frac{{\mathcal{M}_1}^2C_T^2}{2}>0. \tag{3.27}
$$

We note that Λ_3 is postive thanks to (3.14). Then the inequality (3.27) gives

$$
\begin{aligned}
&\left(\frac{1}{2\rho_u}+\Lambda_3+\frac{1+\rho_T}{2}{\mathcal{M}_1}^2C_T^2\right)\|\nabla\mathrm{e}_h^{n+1}\|^2+\frac{\alpha}{2\rho_u}\|\delta_h^{n+1}\|^2+\frac{1+\rho_T^{-1}}{2}\|\nabla\epsilon_h^{n+1}\|^2\\
&\qquad\leq\left(\frac{1}{2\rho_u}+\frac{1+\rho_T}{2}{\mathcal{M}_1}^2C_T^2\right)\|\nabla\mathrm{e}_h^n\|^2+\frac{\alpha}{2\rho_u}\|\delta_h^n\|^2+\frac{1+\rho_T^{-1}}{2}\|\nabla\epsilon_h^n\|^2.
\end{aligned}
\tag{3.28}
$$

Now invoking the induction argument with triangle inequality implies the uniform boundedness of the solution:

$$
\|\nabla\boldsymbol{u}_h^n\|\leq K_u,\ \|\nabla\theta_h^n\|\leq K_\theta,\ \|\nabla T_h^n\|\leq K_T\ \text{and}\ \|p_h^n\|\leq K_p. \tag{3.29}
$$

Moreover, Lemma 3.1 implies that $\lim_{n\to\infty}\|\nabla\mathrm{e}_h^n\|=0$, where we take

$$a_n = \|\nabla \mathrm{e}_h^n\|^2,\ b_n = 0,\ c_n = \frac{\alpha}{2\rho_u}\|\delta_h^n\|^2 + \frac{1+\rho_T^{-1}}{2}\|\nabla \epsilon_h^n\|^2,$$
$$\omega_1 = \frac{1}{2\rho_u} + \Lambda_3 + \frac{1+\rho_T}{2}{\mathcal{M}_2}^2 C_T^2,\ \omega_2 = 1,$$
$$\varepsilon_1 = \Lambda_3,\ \varepsilon_2 = \frac{1}{2}.$$

To show the convergence of other errors, we need to assume that (3.15) holds. Then the buoyancy term error can be bounded as

$$\mathrm{Pr}\,\mathrm{Ra}\, d(\epsilon_h^{n+1}, \mathrm{e}_h^{n+1}) \le \frac{1}{4}\|\nabla \epsilon_h^{n+1}\|^2 + \mathrm{Pr}^2\,\mathrm{Ra}^2 C_p^4 \|\nabla \mathrm{e}_h^{n+1}\|^2, \tag{3.30}$$

instead of (3.26). Setting

$$\widehat{\Lambda}_3 := \widehat{\Lambda}_2 - \rho_T \frac{{\mathcal{M}_2}^2 C_T^2}{2}, \tag{3.31}$$

(3.29) is replaced by

$$\left(\frac{1}{2\rho_u} + \widehat{\Lambda}_3 + \frac{1+\rho_T}{2}{\mathcal{M}_2}^2 C_T^2\right)\|\nabla \mathrm{e}_h^{n+1}\|^2 + \frac{\alpha}{2\rho_u}\|\delta_h^{n+1}\|^2 + \frac{1.5+\rho_T^{-1}}{2}\|\nabla \epsilon_h^{n+1}\|^2 \tag{3.32}$$

$$\le \left(\frac{1}{2\rho_u} + \frac{1+\rho_T}{2}{\mathcal{M}_2}^2 C_T^2\right)\|\nabla \mathrm{e}_h^n\|^2 + \frac{\alpha}{2\rho_u}\|\delta_h^n\|^2 + \frac{1+\rho_T^{-1}}{2}\|\nabla \epsilon_h^{n+1}\|^2, \tag{3.33}$$

which implies that $\lim_{n\to\infty}(\|\nabla \mathrm{e}_h^n\|, \|\nabla \epsilon_h^n\|) = (0,0)$, where we choose

$$a_n = \|\nabla \mathrm{e}_h^n\|^2,\ b_n = \|\nabla \epsilon_h^n\|^2,\ c_n = \frac{\alpha}{2\rho_u}\|\delta_h^n\|^2,$$
$$\omega_1 = \frac{1}{2\rho_u} + \widehat{\Lambda}_3 + \frac{1+\rho_T}{2}{\mathcal{M}_2}^2 C_T^2,\ \omega_2 = \frac{1.5+\rho_T^{-1}}{2},$$
$$\varepsilon_1 = \widehat{\Lambda}_3,\ \varepsilon_2 = \frac{1}{4}.$$

in Lemma 3.1.

The convergence of $\|\delta_h^n\|$ to zero as $n \to \infty$ follows from applying the inf-sup condition in (3.17). □

Theorem 3.3 *(Contractivity) Let $(\mathrm{e}_h^n, \delta_h^n, \epsilon_h^n)$ be as in the Theorem 3.2. If $\widehat{\Lambda}_1 > 0$ and ρ_u, ρ_T are small enough as in (3.15), then there exists $\omega_j > 0$, $j = \overline{1,3}$, and $\kappa \in (0,1)$ such that*

$$\psi_n := \omega_1\|\nabla \mathrm{e}_h^n\|^2 + \omega_2\|\delta_h^n\|^2 + \omega_3\|\nabla \epsilon_h^n\|^2 \tag{3.34}$$

is a contractive sequence, i.e., it satisfies

$$\psi_{n+1} < \kappa\psi_n. \tag{3.35}$$

Proof Let

$$\begin{aligned} &a_n = \|\nabla \mathrm{e}_h^n\|^2,\ b_n = \|\nabla \epsilon_h^n\|^2,\ c_n = \|\delta_h^n\|^2, \\ &\omega_1 = \frac{1}{2\rho_u} + \widehat{\Lambda}_3 + \frac{1+\rho_T}{2}\mathcal{M}_2{}^2 C_T^2,\ \omega_2 = \frac{1.5+\rho_T^{-1}}{2},\ \omega_3 = \frac{\alpha}{2\rho_u}, \\ &\varepsilon_1 = \widehat{\Lambda}_3,\ \varepsilon_2 = 0.25. \end{aligned} \tag{3.36}$$

Then (3.33) is equivalent to (3.7). Moreover, by applying the inf-sup condition in (3.17), we obtain that

$$\|\delta_h^n\| \le \left[\frac{1}{\rho_u} + \mathrm{Pr} + \mathcal{M}_2 K_u + C_p\frac{\rho_u}{\alpha}\right]\|\nabla \mathrm{e}_h^{n+1}\| + \left[\frac{1}{\rho_u} + \mathcal{M}_2 C_u\right]\|\nabla \mathrm{e}_h^n\| + \mathrm{PrRa}C_p^2\|\nabla \epsilon_h^{n+1}\|, \tag{3.37}$$

which is equivalent to (3.8). The proof then directly follows from Lemma 3.2. □

4 Numerical experiments

This section presents numerical experiments designed to test the proposed schemes and validate the theoretical findings. The first example is a standard convergence test using a manufactured exact solution. The second experiment considers a well-known benchmark problem: steady natural convection in a square and cubic cavity for the 2D and 3D cases, respectively [25, 36].

The spatial discretization employs Q2–Q1–Q2 elements for the velocity, pressure, and temperature, respectively. All computations are carried out using `deal.II`, a general-purpose, object-oriented finite element library [2]. For reproducibility purposes, the source code for the experiments below is available at https://github.com/maggul-research/IAH.

For comparison, we also consider two alternative approaches: (i) an alternative AH method (Algorithm 4.1) and (ii) the classical Penalty–Picard Iteration (Algorithm 4.2). The former can be viewed as a variation of Algorithm 3.1 in which the ρ_T terms are omitted, while the latter represents the standard technique widely used for such simulations [6, 29].

Algorithm 4.1. *Alternative Arrow–Hurwicz Method (AAH): Let ρ_u and α be positive parameters, and initialize $(\mathbf{u}_h^0, p_h^0, \theta_h^0) = (\mathbf{0}, 0, 0)$. For $n \geq 0$, find $(\mathbf{u}_h^{n+1}, p_h^{n+1}, \theta_h^{n+1}) \in (\mathbf{X}_h, Q_h, W_h)$ such that, for all $(\mathbf{v}_h, q_h, S_h) \in (\mathbf{X}_h, Q_h, W_h)$,*

$$b_1(\mathbf{u}_h^n, \theta_h^{n+1}, S_h) + (\nabla\theta_h^{n+1}, \nabla S_h) = -b_1(\mathbf{u}_h^n, \widetilde{T}_h, S_h) - (\nabla\widetilde{T}_h, \nabla S_h), \tag{4.1}$$

$$\frac{1}{\rho_u}(\nabla(\mathbf{u}_h^{n+1} - \mathbf{u}_h^n), \nabla\mathbf{v}_h) + \Pr(\nabla\mathbf{u}_h^{n+1}, \nabla\mathbf{v}_h) + b_2(\mathbf{u}_h^n, \mathbf{u}_h^{n+1}, \mathbf{v}_h) - (p_h^n, \nabla\cdot\mathbf{v}_h) + \frac{\rho_u}{\alpha}(\nabla\cdot\mathbf{u}_h^{n+1}, \nabla\cdot\mathbf{v}_h) = \Pr\mathrm{Ra}\, d(\theta_h^{n+1}, \mathbf{v}_h) + \Pr\mathrm{Ra}\, d(\widetilde{T}_h, \mathbf{v}_h), \tag{4.2}$$

$$\alpha(p_h^{n+1} - p_h^n, q_h) + \rho_u(\nabla\cdot\mathbf{u}_h^{n+1}, q_h) = 0. \tag{4.3}$$

Algorithm 4.2. *Penalty–Picard Iteration (PPI): Let $\beta > 0$ and initialize $(\mathbf{u}_h^0, p_h^0, \theta_h^0) = (\mathbf{0}, 0, 0)$. For $n \geq 0$, find $(\mathbf{u}_h^{n+1}, p_h^{n+1}, \theta_h^{n+1}) \in (\mathbf{X}_h, Q_h, W_h)$ such that, for all $(\mathbf{v}_h, q_h, S_h) \in (\mathbf{X}_h, Q_h, W_h)$,*

$$b_1(\mathbf{u}_h^n, \theta_h^{n+1}, S_h) + (\nabla\theta_h^{n+1}, \nabla S_h) = -b_1(\mathbf{u}_h^n, \widetilde{T}_h, S_h) - (\nabla\widetilde{T}_h, \nabla S_h), \tag{4.4}$$

$$\Pr(\nabla\mathbf{u}_h^{n+1}, \nabla\mathbf{v}_h) + b_2(\mathbf{u}_h^n, \mathbf{u}_h^{n+1}, \mathbf{v}_h) - (p_h^n, \nabla\cdot\mathbf{v}_h) + \beta(\nabla\cdot\mathbf{u}_h^{n+1}, \nabla\cdot\mathbf{v}_h) = \Pr\mathrm{Ra}\, d(\theta_h^{n+1}, \mathbf{v}_h) + \Pr\mathrm{Ra}\, d(\widetilde{T}_h, \mathbf{v}_h), \tag{4.5}$$

$$\frac{1}{\beta}(p_h^{n+1} - p_h^n, q_h) + (\nabla\cdot\mathbf{u}_h^{n+1}, q_h) = 0. \tag{4.6}$$

4.1 Convergence test

In this subsection, we present the convergence rate results. To begin, we consider the following two-dimensional manufactured (exact) solution to the continuous problem defined on the domain $\Omega = [0,1] \times [0,1]$:

$$\boldsymbol{u} = \begin{pmatrix} y^3 \\ x^3 \end{pmatrix}, \qquad T = \frac{3}{2\mathrm{PrRa}}\,(2x^2y^3 - x^4y), \qquad p = 6\mathrm{Pr}\,xy - \frac{3}{4}x^4y^2. \tag{4.7}$$

This manufactured solution is selected such that the velocity field is solely influenced by the temperature, which is driven by an external force. Boundary conditions are strongly enforced to coincide with the exact solution on all boundaries.

The parameter values used in this test are $\mathrm{Pr} = 1$, $\mathrm{Ra} = 1000$, $\rho_u = 100$, $\rho_T = 10$, $\alpha = 0.1$, and $\beta = 1000$. A uniform mesh of size $h = 1/2^N$ is employed, where N denotes the mesh refinement level. The iterative process is terminated once the following stopping criterion is satisfied for a tolerance $\tau = 10^{-6}$:

$$\max\left\{\frac{\|\boldsymbol{u}_h^{n+1} - \boldsymbol{u}_h^n\|}{\|\boldsymbol{u}_h^{n+1}\|}, \frac{\|\theta_h^{n+1} - \theta_h^n\|}{\|\theta_h^{n+1}\|}, \frac{\|p_h^{n+1} - p_h^n\|}{\|p_h^{n+1}\|}\right\} \leq \tau. \tag{4.8}$$

For the proposed IAH method (Algorithm 3.1), we expect to achieve second-order accuracy in the $H^1(\Omega)$ semi-norm of the errors and third-order accuracy in the $L^2(\Omega)$ norm of the errors. summarized in Table 1rates, summarized in Table 1 for IAH method (similar results are obtained for AAH and PPI in both two and three dimensions), confirm these theoretical expectations.

Secondly, we perform a three-dimensional convergence analysis. To this end, we consider the following exact (manufactured) solution, defined on the domain $\Omega = [0,1] \times [0,1] \times [0,1]$ and using the same parameter values as in the two-dimensional test:

Table 1 Errors and Convergence Rates in 2D

		Errors and CRs in u				Errors and CRs in T			
N	DoFs (u, T)	$\|\|u-u^h\|\|$	CR	$\|\|\nabla u-\nabla u^h\|\|$	CR	$\|\|T-T^h\|\|$	CR	$\|\|\nabla T-\nabla T^h\|\|$	CR
2	162,81	6.68230e−04	-	2.82085e−02	-	1.13127e−06	-	4.80462e−05	-
3	578,289	8.35291e−05	3.00	7.05212e−03	2.00	1.42030e−07	2.99	1.20099e−05	2.00
4	2178,1089	1.04411e−05	3.00	1.76303e−03	2.00	1.77737e−08	3.00	3.00237e−06	2.00
5	8450,4225	1.30514e−06	3.00	4.40758e−04	2.00	2.22235e−09	3.00	7.50585e−07	2.00
6	33282,16641	1.63142e−07	3.00	1.10189e−04	2.00	2.77814e−10	3.00	1.87646e−07	2.00
7	132098,66049	2.03928e−08	3.00	2.75473e−05	2.00	3.47274e−11	3.00	4.69114e−08	2.00
8	526338,263169	2.54910e−09	3.00	6.88683e−06	2.00	4.34094e−12	3.00	1.17279e−08	2.00

Table 2 Errors and Convergence Rates in 3D

		Errors and CRs in u				Errors and CRs in T			
N	DoFs (u, T)	$\|\|u-u^h\|\|$	CR	$\|\|\nabla u-\nabla u^h\|\|$	CR	$\|\|T-T^h\|\|$	CR	$\|\|\nabla T-\nabla T^h\|\|$	CR
2	2187,729	5.63649e−02	-	2.07844e−00	-	3.95800e−04	-	6.39580e−03	-
3	14739,4913	6.72006e−03	3.06	5.11922e−01	2.02	4.25569e−05	3.21	7.18561e−04	3.15
4	107811,35937	7.97709e−04	3.07	1.26426e−01	2.01	4.88796e−06	3.12	7.32771e−05	3.29
5	823875,274625	9.55344e−05	3.06	3.13547e−02	2.01	4.54229e−07	3.42	6.62369e−06	3.46

$$\boldsymbol{u} = \begin{pmatrix} ay^2 \\ 0 \\ ax^3 \end{pmatrix}, \qquad T = \frac{3a^2x^2y^2 - 6ax\mathrm{Pr}}{\mathrm{PrRa}}, \qquad p = 2ax\mathrm{Pr}, \qquad a = 100. \quad (4.9)$$

The errors and corresponding convergence rates, reported in Table 2 for IAH method, align well with our theoretical predictions. As in the two-dimensional case, the method achieves a second-order of accuracy in $H^1(\Omega)$ semi-norm and third-order of accuracy in $L^2(\Omega)$ norm of the errors. It is worth noting that the temperature errors exhibit slightly higher convergence rates, indicating a mild super convergence behavior.

4.2 Steady natural convection in a square/cubic cavity

We now present numerical results for steady natural convection in both a square [20, 23, 25, 36] and a cubic cavity [17, 19]. Following the standard benchmark configurations, we compare our results with those available in the literature. The results obtained with IAH, AAH and PPI are reported for both the two- and three-dimensional cases.

In this setup, fluid motion is driven by differentially heated vertical walls. The Prandtl number is fixed at $\mathrm{Pr} = 0.71$, while computations are performed for Rayleigh numbers ranging from 10^3 to 10^8. The stopping criterion follows (4.8) with a tolerance of $\tau = 10^{-4}$. The problem parameters, iteration counts, and computation times required to achieve the prescribed tolerance for the 2D and 3D simulations are summarized in Tables 3 and 4, respectively.

Table 3 Number of Iterations and Computation Time in 2D

Ra	10^3	10^4	10^5	10^6	10^7	10^8
# of iters with IAH	84	77	76	83	252	1690
computation time IAH	13 m	13 m	13 m	15 m	43 m	4 h:16 m
# of iters with AAH	88	79	80	*	*	*
computation time AAH	13 m	13 m	14 m	*	*	*
# of iters with PPI	6	*	*	*	*	*
computation time PPI	11 m	*	*	*	*	*

* does not converge

Table 4 Number of Iterations and Computation Time in 3D

Ra	10^3	10^4	10^5	10^6	10^7
#of iters with IAH	88	78	80	99	258
computation time IAH	4 h:30 m	4 h:23 m	4 h:27 m	5 h:30 m	16 h:11 m
#of iters with AAH	91	81	81	*	*
computation time AAH	4 h:39 m	4 h:21 m	4 h:38 m	*	*
#of iters with PPI	5	*	*	*	*
computation time PPI	2 h:32 m	*	*	*	*

* does not converge

The parameter selection process follows a systematic strategy. For the alternative method AAH, the parameters α and ρ_u were chosen to ensure stable and robust convergence across a wide range of Rayleigh numbers, leading to the choice $\alpha = 10^{-4}$ and $\rho_u = 10^{-1}$. These values were then fixed for both proposed IAH and AAH, while the remaining parameter was set to $\rho_T = 2 \times 10^{-1}$. This choice intentionally favors AAH to demonstrate that IAH maintains superior performance even under conditions where AAH already converges reliably. Additionally, $\beta = 1000$ was selected for PPI in this study.

Under these settings, however, AAH fails to converge for $\mathrm{Ra} = 10^6$, whereas IAH continues to converge up to $\mathrm{Ra} = 10^8$ in two dimensions and $\mathrm{Ra} = 10^7$ in three dimensions. To achieve convergence at such high Rayleigh numbers, ρ_T was reduced to 2×10^{-2} and 2×10^{-3} for $\mathrm{Ra} = 10^7$ and $\mathrm{Ra} = 10^8$, respectively. This corresponds to a parameter refinement strategy in which ρ_T decreases by an order of magnitude as *Ra* increases by the same factor. Furthermore, these results reveal a clear pattern: maintaining the ratio $\rho_u/\alpha = 10^3$ is crucial for achieving rapid convergence, while ρ_T should be progressively reduced in proportion to increasing Ra.

4.2.1 Square cavity

In the two-dimensional case, the computational domain consists of a square cavity with vertically oriented walls that are differentially heated to induce fluid motion. Specifically, the left wall is maintained at a hot temperature, while the right wall is kept cold. The horizontal walls are thermally insulated, thereby preventing heat transfer across them. No-slip boundary conditions are imposed for the velocity field on all walls, i.e., $\boldsymbol{u}(x, y) = 0$. For the temperature, Dirichlet boundary conditions are prescribed on the vertical walls as $T(x, y) = 1 - x$, while adiabatic (Neumann) boundary conditions, $\nabla T \cdot \mathrm{n} = 0$, are applied on the horizontal walls. All computations are carried out on the uniform coarse mesh shown in Fig. 1, with a mesh size of $h = 1/64$.

As shown in Table 3, AAH method fails to converge beyond $\mathrm{Ra} = 10^5$. In contrast, IAH successfully converges and provides reliable results even at $\mathrm{Ra} = 10^7$ and $\mathrm{Ra} = 10^8$. It is important to note that, at such high Rayleigh numbers, the small-data assumptions underlying the theoretical analysis are no longer strictly valid; nevertheless, the desired convergence is still achieved. These results highlight the robustness and effectiveness of the proposed algorithm, which maintains stability and accuracy under challenging conditions. By comparison, AAH fails to converge for $\mathrm{Ra} = 10^6$, and PPI breaks down at considerably lower Rayleigh numbers, consistently failing for $\mathrm{Ra} \geq 10^4$.

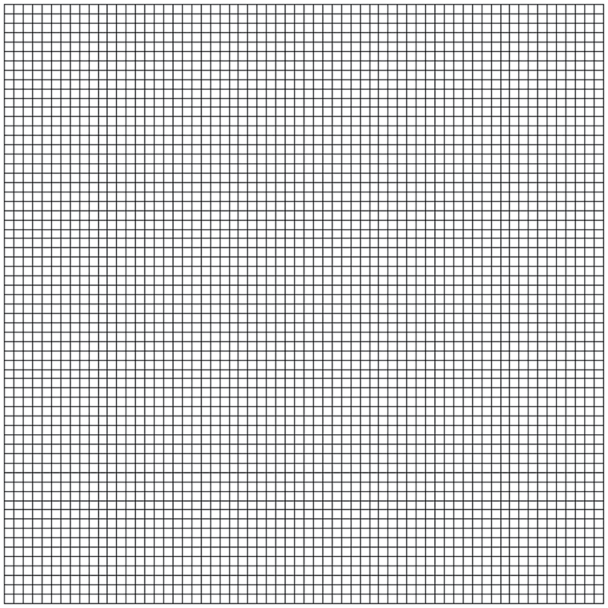

Fig. 1 2D Mesh for $h = 1/64$

Table 5 Comparison with the reference values of [36]

Ra	10^3	10^4	10^5	10^6	10^7	10^8
$u_{1,max}^{ref}$	3.6434	15.967	33.51	65.55	145.06	295.67
y_{ref}	0.8167	0.8167	0.85	0.86	0.92	0.94
$u_{1,max}^{IAH}$	3.6475	16.1775	34.7123	64.4707	145.705	313.492
y_{IAH}	0.8125	0.8281	0.8594	0.8437	0.8750	0.9375
$u_{1,max}^{AAH}$	3.6459	16.1744	34.6863	*	*	*
y_{AAH}	0.8125	0.8281	0.8594	*	*	*
$u_{1,max}^{PPI}$	3.6495	*	*	*	*	*
y_{PPI}	0.8125	*	*	*	*	*
$u_{2,max}^{ref}$	3.686	19.98	70.81	227.24	714.47	2290.13
x_{ref}	0.183	0.117	0.070	0.040	0.021	0.013
$u_{2,max}^{IAH}$	3.6899	19.6044	68.5285	215.533	658.554	2065.66
x_{IAH}	0.1719	0.125	0.0625	0.0312	0.0156	0.01562
$u_{2,max}^{AAH}$	3.6893	19.6053	68.5158	*	*	*
x_{AAH}	0.1719	0.125	0.0625	*	*	*
$u_{2,max}^{PPI}$	3.6944	*	*	*	*	*
y_{PPI}	0.1719	*	*	*	*	*

* does not converge

The comparison results with the benchmark study [36] are summarized in Table 5. The listed quantities are introduced to validate the present numerical results against the reference data. Let $u_i = \boldsymbol{u} \cdot \mathrm{e}_i$ for $i = 1, 2$, where e_i are the standard basis vectors. We define

$$u_{1,\max}^{\lambda} := u_1(0.5, y_\lambda) = \max_y \left\{u_1^{\lambda}(0.5, y)\right\}, \qquad u_{2,\max}^{\lambda} := u_2(x_\lambda, 0.5) = \max_x \left\{u_2^{\lambda}(x, 0.5)\right\},$$

where $\lambda = \mathrm{ref}$ denotes the reference values from [36], and $\lambda = \mathrm{AAH}, \mathrm{IAH}, \mathrm{PPI}$ correspond to the results obtained using Algorithms 3.1, 4.1, and 4.2, respectively.

Table 5 demonstrates the strong agreement between the present results and the benchmark data reported in [36]. All three algorithms yield nearly identical results in cases where AAH and PPI achieve convergence. In regimes where convergence is obtained only with IAH, the results remain in close agreement with the reference values.

A qualitative comparison with the reference visualizations further confirms this consistency. Because the plots produced by all three algorithms are visually indistinguishable, only the results obtained using AAH are presented here. The contour plots of velocity magnitude, velocity components ($x-$ and $y-$), and temperature fields exhibit excellent agreement with the patterns reported in the literature, [25, 36].

4.2.2 Cubic cavity

Similarly, in the three-dimensional case, the computational domain consists of a cubic cavity with vertically oriented sidewalls that are differentially heated. The left and right walls are maintained at hot and cold temperatures, respectively, while the remaining four walls (front, back, top, and bottom) are thermally insulated to prevent any heat transfer. Homogeneous no-slip velocity boundary conditions are enforced on all six walls. For the temperature field, Dirichlet boundary conditions are prescribed on the vertical sidewalls as $T(x, y, z) = 1 - x$, while adiabatic (Neumann) boundary conditions, $\nabla T \cdot \mathrm{n} = 0$, are applied on the remaining walls.

The same parameter sets used in the two-dimensional study are adopted here. As shown in Table 4, the number of iterations required for convergence closely matches those of the 2D simulations. The computations are performed on a uniform mesh with mesh size $h = 1/32$, as illustrated in Fig. 2. Despite this relatively coarse resolution, corresponding to a total of 1,134,437 degrees of freedom, the numerical results exhibit strong agreement with the reference visualizations reported in [17].

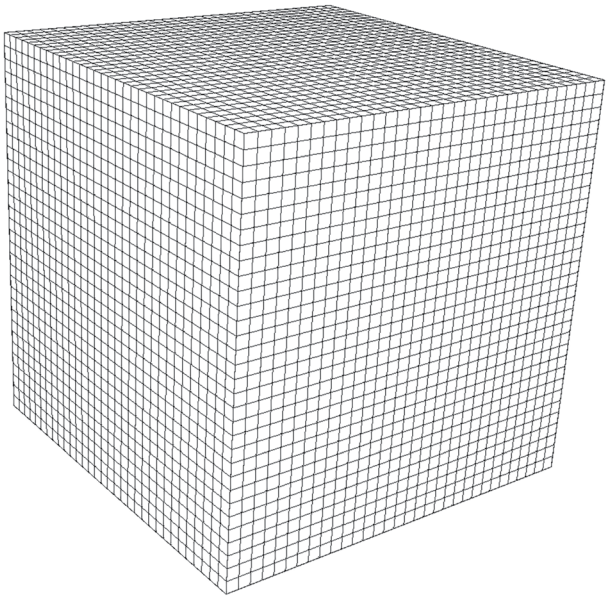

Fig. 2 3D Mesh for $h = 1/32$

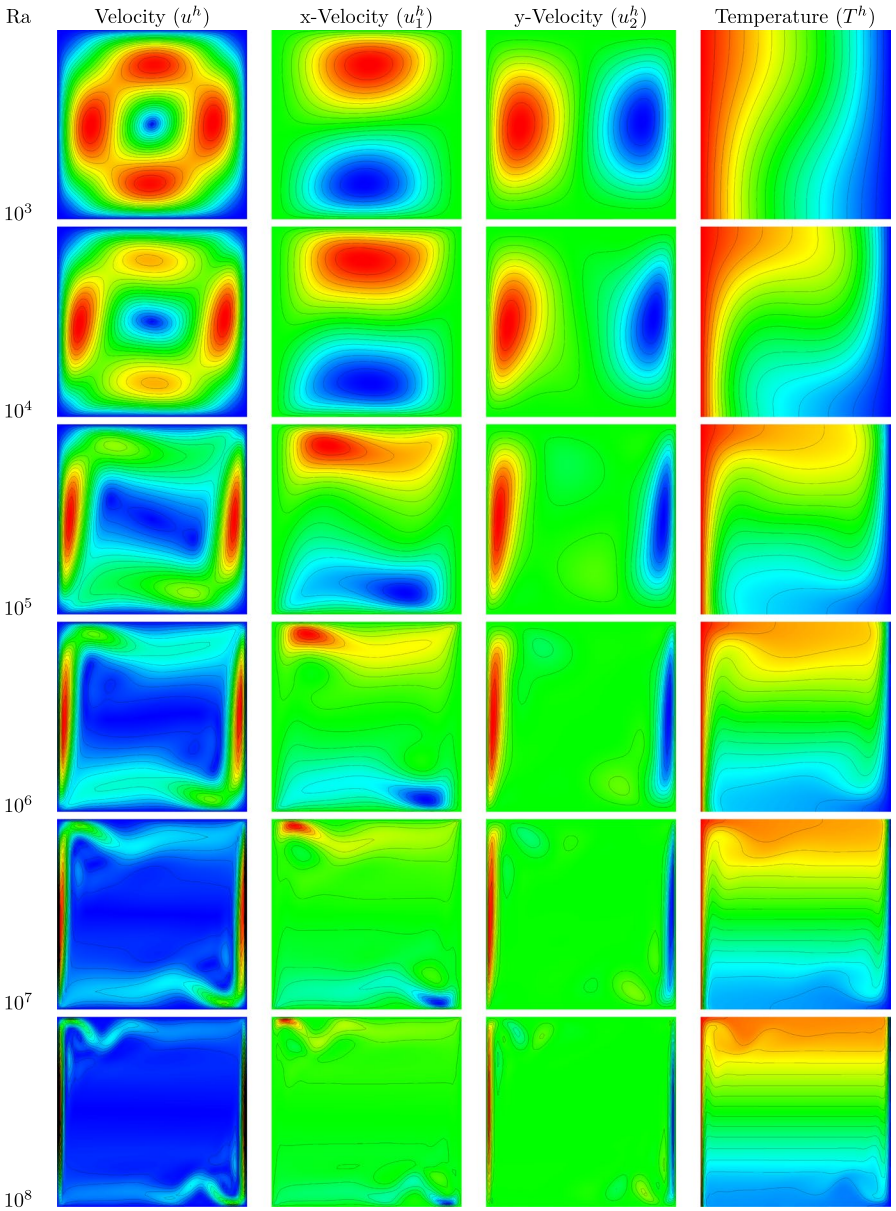
Ra
Velocity (u^h)
x-Velocity (u_1^h)
y-Velocity (u_2^h)
Temperature (T^h)
10^3
10^4
10^5
10^6
10^7
10^8

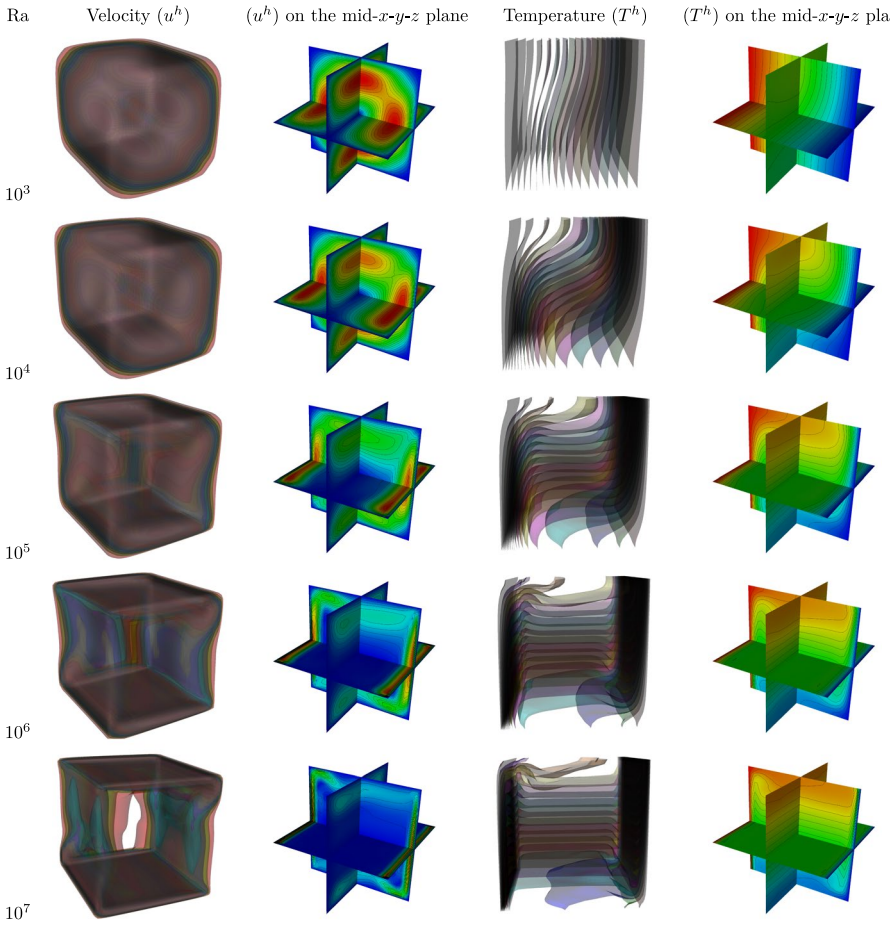

5 Conclusion

In this work, we developed and analyzed an Improved Arrow–Hurwicz (IAH) method for the steady Boussinesq equations with nonhomogeneous partitioned Dirichlet boundary conditions. By introducing an AH–type update for the temperature equation, we established that the proposed formulation overcomes the limitations of the classical Arrow–Hurwicz approach when applied solely to the momentum equation. This modification is essential for achieving robust convergence in buoyancy-driven flows, particularly in high–Rayleigh number regimes where continuation strategies are typically required.

We proved existence, uniqueness, uniform boundedness, and convergence of the finite element approximation under standard small-data assumptions, and derived

error estimates for the discrete scheme. The resulting algorithm is fully decoupled and avoids solving saddle-point systems at each iteration, leading to a computationally efficient alternative to classical projection-type and penalty-based methods.

Comprehensive two- and three-dimensional numerical experiments demonstrated the accuracy and efficiency of the IAH method, confirming superior performance compared to the alternative AH scheme and the Penalty–Picard iteration. In particular, the proposed approach consistently achieved stable convergence at high Rayleigh numbers, highlighting its effectiveness as a scalable solver for steady natural convection.

Future work includes the extension of the method to adaptive mesh refinement strategies, and the development of accelerated variants incorporating multilevel or Anderson acceleration techniques. The analysis and computational evidence presented here show that the improved Arrow–Hurwicz method provides a promising framework for efficient solution of more complex thermally driven incompressible flow systems.

Funding Open access funding provided by SCELC, Statewide California Electronic Library Consortium. The first author would like to acknowledge the support from a University of Sharjah grant No. 22021440125.

Data availability This study has no associated data to be shared. For reproducibility purposes, the source code for the experiments is available at https://github.com/maggul-research/IAH

Declarations

Conflict of interest The authors declare that they have no conflict of interest.

References

1. Arrow, K.J., Hurwicz, L.: Gradient method for concave programming I: Local results. In: Arrow, K.J., Hurwicz, L., Uzawa, H. (eds.) Studies in Linear and Nonlinear Programming, pp. 117–126. Stanford University Press, Stanford, CA (1958)
2. Bangerth, W., Davydov, D., Heister, T., Heltai, L., Kanschat, G., Kronbichler, M., Maier, M., Turcksin, B., Wells, D.: The deal.II Library, Version 8.4. J. Numer. Math. **24**(3), 135–141 (2016)
3. Boland, J., Layton, W.: Error analysis for finite element methods for steady natural convection problems. Numer. Funct. Anal. Optim. **11**(5–6), 449–483 (1990)
4. Brizitskii, R.V., Saritskaia, Z.Y.: Analysis of inhomogeneous boundary value problems for generalized Boussinesq model of mass transfer. J. Dyn. Control Syst. **29**, 1809–1828 (2023)
5. Chen, P., Huang, J., Sheng, H.: Solving steady incompressible Navier-Stokes equations by the Arrow-Hurwicz method. J. Comput. Appl. Math. **311**, 100–114 (2017)

6. Codina, R.: An iterative penalty method for the finite element solution of the stationary Navier-Stokes equations. Comput. Methods Appl. Mech. Engrg. **110**, 237–262 (1993)
7. Colmenares, E., Neilan, M.: Dual-mixed finite element methods for the stationary Boussinesq problem. Comput. Math. Appl. **72**(7), 1828–1850 (2016)
8. Deteix, J., Yakoubi, D.: An iterative split scheme for steady flows with heterogeneous viscosity. Comput. Methods Appl. Mech. Engrg. **432**, 117391 (2024)
9. Fiordilino, J.A., Pakzad, A.: A discrete Hopf interpolant and stability of the finite element method for natural convection. Math. Comput. **89**, 629–643 (2020)
10. Geredeli, P., Rebholz, L.G., Vargun, D., Zytoon, A.: Improved convergence of the Arrow-Hurwicz iteration for the Navier-Stokes equation via grad-div stabilization and Anderson acceleration. J. Comput. Appl. Math. **422**, 114920 (2023)
11. Girault, V., Raviart, P.-A., *Finite Element Methods for Navier-Stokes Equations: Theory and Algorithms*. Springer Series in Computational Mathematics, (5). Springer, Berlin,(1986)
12. He, B., Xu, S., Yuan, X.: On convergence of the Arrow-Hurwicz Method for saddle point problems. J. Math. Imaging Vis. **64**, 662–671 (2022)
13. Herrero, H., Hoyas, S., Donoso, A., Mancho, A.M.A.M., Chacón, J.M., Portugués, R.F., Yeste, B.: Chebyshev collocation for a convective problem in primitive variable formulation. J. Sci. Comput. **18**(3), 315–328 (2003)
14. Herrero, H., Pla, F., Ruiz-Ferrández, M.: A Schwarz method for a Rayleigh-Bénard problem. J. Sci. Comput. **78**(1), 376–392 (2019)
15. Keram, A., Huang, P.: The Arrow-Hurwicz iterative finite element method for the stationary thermally coupled incompressible magnetohydrodynamics flow. J. Sci. Comput. **92**, 11 (2022)
16. Lai, D., Huang, P., He, Y.: One- and two-level Arrow–Hurwicz-type iterative algorithms for the stationary Smagorinsky model. Commun. Nonlinear Sci. Numer. Simul. **134**, 108001 (2024)
17. Lee, H.S., Jung, J.H., Yoon, H.S.: A numerical study of three- dimensional natural convection in a differentially heated cubical enclosure. International Journal of Energy **14**, (2020)
18. Lorca, S.A., Boldrini, J.L.: Stationary solutions for generalized Boussinesq models. J. Differential Equations **124**(2), 389–406 (1996)
19. Mallinson,G.D.,De Vahl Davis ,G., Three-dimensional natural convection in a box: a numerical study. *Journal of Fluid Mechanics*, 83(1):1–31, (1977)
20. Manzari, M.T., An explicit finite element algorithm for convection heat transfer problems. *Int. J. Numer. Methods Heat Fluid Flow*, 9(8):860–877, (1999)
21. Marques, G.M.,Wells,M.G.,Padman, L.,özgökmen, T.M., Flow splitting in numerical simulations of oceanic dense-water outflows. *Ocean Modell.*, 113:66–84, 2017
22. Martínez, D., Pla, F., Herrero, H., Fernández-Pérez, A.: A Schwarz alternating method for an evolution convection problem. Appl. Numer. Math. **192**, 179–196 (2023)
23. Mayne,D.A., Usmani, A.S., Crapper, M., h-adaptive finite element solution of high Rayleigh number thermally driven cavity problem. *Int. J. Numer. Meth. Heat Fluid Flow*, 10(6):598–615, (2000)
24. Mellado, J.P.: Using numerical simulations to study the atmospheric boundary layer. In: García-Villalba, M., Kuerten, H., Salvetti, M.V. (eds.) Direct and Large Eddy Simulation XII. pp, pp. 1–10. Springer International Publishing, Cham (2020)
25. Moore, E.F., Davis, R.W.: Numerical Solutions for Steady Natural Convection in a Square Cavity. Commerce Department, National Institute of Standards and Technology (NIST) (1984)
26. Morimoto, H., On non-stationary $Boussinesq$ equations. *Proc. Japan Acad. Ser. A Math. Sci.*, 67(5):159 – 161, 1991
27. Oyarzúa, R., Qin, T., Schötzau, D.: An exactly divergence-free finite element method for a generalized Boussinesq problem. IMA J. Numer. Anal. **34**(3), 1104–1135 (2014)
28. Oyarzúa, R., Zúñiga, P.: Analysis of a conforming finite element method for the Boussinesq problem with temperature-dependent parameters. J. Comput. Appl. Math. **323**, 71–94 (2017)
29. Pollock, S., Rebholz, L.G., Xiao, M.: Acceleration of nonlinear solvers for natural convection problems. J. Numer. Math. **29**(4), 323–341 (2021)
30. Scott, R., Zhang, S.: Finite element interpolation of nonsmooth functions satisfying boundary conditions. Math. Comput. **54**(190), 483–493 (1990)
31. Scurtu, N., Futterer, B., Egbers, C.: Pulsating and traveling wave modes of natural convection in spherical shells. Phys. Fluids **22**(11), 114108 (2010)
32. Tabata, M., Tagami, D.: Error estimates of finite element methods for nonstationary thermal convection problems with temperature-dependent coefficients. Numer. Math. **100**, 351–372 (2005)

33. Takhirov, A., Cıbık, A., Eroglu, F.G., Kaya, S.: An improved Arrow-Hurwicz method for the steady-state Navier-Stokes equations. J. Sci. Comput. **96**, 52 (2023)
34. Takhirov, A., Frolov, R., Minev, P.: A direction splitting scheme for Navier-Stokes-Boussinesq system in spherical shell geometries. Int. J. Numer. Methods Fluids **93**, 3507–3523 (2021)
35. Temam, R.: Navier-Stokes Equations: Theory and Numerical Analysis. North Holland (1979)
36. D. C. Wan, B. S. V. Patnaik, and G. W. Wei. A new benchmark quality solution for the buoyancy-driven cavity by discrete singular convolution. *Numer. Heat Transfer, Part B: Fundamentals*, 40(3):199–228, 2001
37. Yang, Y., Jiang, Y.L., Kong, Q.X.: The Arrow-Hurwicz iterative finite element method for the stationary magnetohydrodynamics flow. Appl. Math. Comput. **356**, 347–361 (2019)

Authors and Affiliations

Aziz Takhirov[1] · Mustafa Aggul[2,3,4] · Sinan Ergen[5,6] · Fatma G. Eroglu[7] · Songül Kaya[8]

✉ Mustafa Aggul
maggul@umbc.edu

Aziz Takhirov
atakhirov@sharjah.ac.ae

Sinan Ergen
sinan.ergen@balikesir.edu.tr

Fatma G. Eroglu
fatma.guler@atilim.edu.tr

Songül Kaya
smerdan@metu.edu.tr

1 Department of Mathematics, University of Sharjah, Sharjah, UAE

2 Department of Mathematics and Statistics, University of Maryland, Baltimore, MD 21250, USA

3 Department of Mathematics, Southern Methodist University, Dallas, TX 75205, USA

4 Department of Mathematics, Hacettepe University, Ankara 06800, Turkey

5 Department of Mathematics, Balikesir University, Balikesir 10145, Turkey

6 Department of Mathematics, Hacettepe University, Ankara 06800, Turkey

7 Department of Mathematics, Atilim University, Ankara 06830, Turkey

8 Department of Mathematics, Middle East Technical University, Ankara 06800, Turkey